

WIND TUNNEL AND CFD STUDY OF AIRFOIL WITH AIRBRAKE

Pátek Z.* , Červinka J.* , Vrchota P.*

***Aeronautical Research and Test Establishment, Prague, Czech Republic
patek@vzlu.cz; cervinka@vzlu.cz; vrchota@vzlu.cz**

Keywords: *Airbrake, wind tunnel test, CFD*

Abstract

Study of aerodynamics of an airbrake positioned on upper side of a generic laminar sailplane airfoil section was performed using low-speed wind tunnel testing and CFD, including the study of influence of a gap between the airfoil upper surface and the bottom edge of the airbrake. Forces and moments testing, surface pressure distributions and flow visualizations using PIV and mini-tufts were performed.

The results of the study enable to better understand the details of aerodynamic phenomena connected with the airbrake including related flow physics. The results enable to better predict an airbrake performance and to better estimate the influence of airbrake on the other parts of an aircraft. The results also constitute validation case embodying complex flow physics for 2D CFD codes.

1 Introduction and motivation

An airbrake (also called dive brake or speed brake or aerodynamic brake) is a device currently used to control glide path of the sailplanes and motorgliders, namely in the final approach stage of the flight. The necessity of its use is given by high lift-to-drag ratio of these aircraft that makes exact final approach very uneasy without airbrakes. As today secondary role (but historically primary reason for the airbrake invention and introduction), the airbrake shall prevent exceeding of certificated never exceed speed. The principal air-

brake effects are evident, decreasing of the lift and increasing of the drag. Surprisingly, detailed description and explanation of the flow physics as well as quantitative values are difficult to find in the available literature sources. The reasons consist in the fact that main research activities were performed in connection with military dive aircraft, in the thirties of the last century, and airbrake use at that time was different from their current use, the technical design of airbrakes also has changed.

The airbrakes were firstly proposed by Jacobs [1][2] especially as a safety device to limit speed in anomalous flight positions following disorientation or an error of a pilot, although the possibility of their using to facilitate landing was mentioned. Jacobs fundamental articles presented speed polar for a complete aircraft with DFS-type airbrakes and 2D smoke wind tunnel visualization for three airbrake configurations, without providing any aerodynamic forces or pressure data. Hoerner [3] was very brief, focused on the influence on drag only, he did not pay attention to the explanation of the flow physics and did not cover the type of the airbrake that would be interesting for contemporary sailplane design. Rebuffet [4] gave more considerations on the general performance including lift and moment consequences of plate airbrake similar to the current sailplane airbrakes, but did not bring nor pressure distributions, nor description of the connected flow phenomena. Schlichting and Truckenbrodt [5] presented basic valuable information on a airbrake similar to the currently used type,

but general survey character of the book did not bring detailed descriptions. Fuchs [6] performed systematic wind tunnel study of airbrakes on a model of an aircraft with elliptical wing and on a model of a rectangular wing. The main purpose, also in this study, was to provide data for control of dive flight of military aircraft. In addition to force results, Fuchs presented also pressure distributions for one airbrake configuration, unfortunately for the airbrake positioned only on the lower side of the wing, the configuration not used anywise on current aircraft. Davies' report [7] contained more quantitative information including influence on lift and trim of larger spectrum of airbrake types, but described flaps also were not of current sailplane type, although the airbrakes of Hamilcar WW II military glider could be at least of certain interest. However the presented results were limited on global aerodynamic forces, without any airfoil pressure distributions and mainly without descriptions of flow physics and its specific phenomena. Arnold [8] dealt with force and moment measurements of finite-span wing with airbrakes of different relative span. Airbrakes on the upper surface, the lower surface and the both surfaces were studied, also influence of the brake height, brake chordwise position and the gap between the airfoil and airbrake were examined to the certain extent.

The mentioned literature results were connected primordially either with very specific kind of past military flying and thus focused mainly on speed control during steep dive either with prevention of exceeding of permitted speed. They are not directly exploitable for design of contemporary sailplanes or light aircraft, mainly due to the substantial differences in wing airfoil sections, in airbrake configurations and due to current use as the control devices of the slope of relatively shallow flight path (shallow compared to military dive attack) at practically constant low speed.

2 Model

A model of an advanced generic sailplane airfoil section was used. The model was in the form of

rectangular wing with circular endplates (Fig. 1). Maximum thickness of the airfoil was 14.5 percent of the chord, positioned at 43.5 percent of the chord. The pressure distributions were taken using 68 pressure taps.



Fig. 1 Model equipped with the airbrake in the test section

The airbrake was of the Schempp-Hirth type that is almost the only type used on current sailplanes. Its model consisted of a plate perpendicular to the airfoil chord equipped with short perpendicular ledge on the upper edge (Fig. 2). This ledge simulated spring-loaded cap covering the airbrake plate and assuring smooth wing surface contour with the airbrake in retracted position.

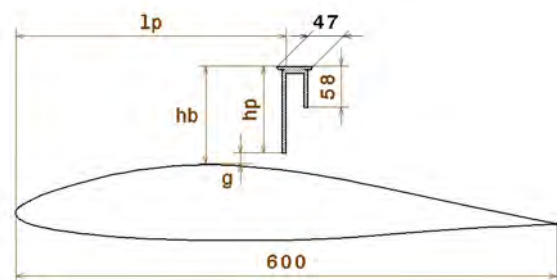


Fig. 2 Airbrake geometry

3 Wind tunnel and measuring devices

The tests were performed in the 3m LSWT low speed wind tunnel at VZLU, Aeronautical Re-

search and Test Establishment in Prague. The wind tunnel used was an atmospheric type with open test section of 3 meter diameter [9]. The model was hinged on a balance to measure lift, drag and pitching moment. The surface pressure distributions were measured using pressure block built into the model.

Particle Image Velocimetry (PIV) experiment was conducted to better understand the development of flowfield in two distinct cases, the airbrake with and without a gap between the airfoil upper side and the airbrake bottom edge.

Visualization of boundary layer flow was performed using minitufts illuminated by ultraviolet light.

The Reynolds number based on the airfoil chord was $Re = 1.5 \cdot 10^6$.

4 Mesh generator and Flow Solver

A hybrid unstructured grid with prismatic layers, defining the airfoil geometry and simulating the boundary layer, was used due to the simplicity of creating such grids on complex geometries. Only one mesh was generated for all cases using a commercial software package ICEM CFD to create an Euler mesh that is used as input to meshing program TRITET [10] that generates a suitable mesh for Reynolds-averages Navier-Stokes (RANS) computations. The near-wall grid spacing normal to the wall was set to be less than 2.5×10^{-6} chord of the main airfoil (c) to obtain $y^+ \approx 1$ based on turbulent flap plate boundary-layer thickness estimate at the Reynolds number in question. The mesh was refined in some regions of interest especially in close proximity of the actuators and the flap. This refinement was used to capture the flow stream from the actuators and wakes behind the airfoil and the flap.

The RANS equations are solved in EDGE, FOI's in-house computational fluid dynamic (CFD) program package [11]. It is a finite volume Navier-Stokes solver for unstructured meshes. It employs local time-stepping, local low-speed preconditioning, multigrid and dual-time-stepping for steady-state and time-dependent problems. The data structure is edge-

based so that the code is constructed as cell-vertex. Convergence is accelerated by pseudo-time stepping and full multigrid.

Due to the massive flow separation behind the airbrake, the calculation was done in unsteady mode. The time step was adjusted according to CFL number to satisfy stability condition.

The Hellsten $k-\omega$ explicit algebraic Reynolds-stress turbulence model [12] was used for this study.

5 Results

5.1 Fundamental airbrake aerodynamics

The airbrake itself created a barrier perpendicular to the flow, the airfoil became extremely asymmetric. The aerodynamic consequences of such obstacle were significantly pronounced in strong asymmetry of the flowfield.

The PIV measurement and minituft surface visualization in the proximity of the leading edge clearly showed the differences in flow pattern. With the airbrake extended, the flow on upper side was slowed down and the stagnation point moved to upper surface, the flow going down was forced to overcome small curvature of the leading edge and thus it was vulnerable to leading edge separation (see Fig. 3 and Fig. 4).

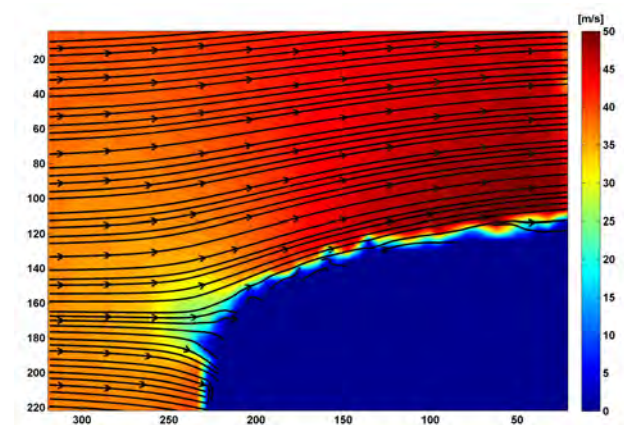


Fig. 3 PIV Leading edge, airbrake retracted

Upstream of the airbrake, the upper side of the airfoil was characterized by pronounced overpressure even at positive angles of attack. A separated area extended approximately 15 percent of

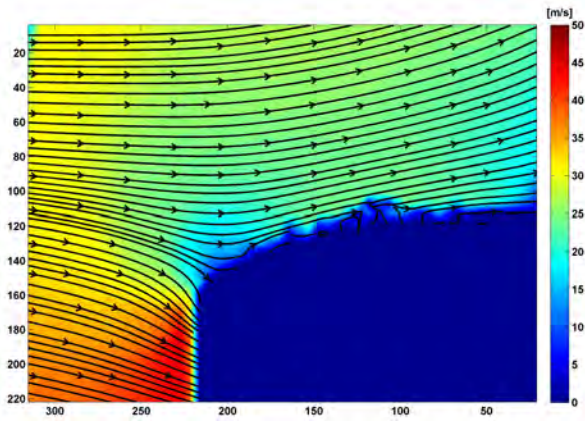


Fig. 4 PIV Leading edge, airbrake extended, gap 0

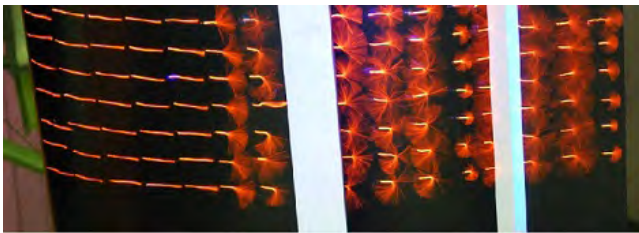


Fig. 5 Upper side, the extended airbrake is a broader light band in the middle of airfoil, gap 0, AoA 0deg

the airfoil chord downstream of the airbrake and slowly expanded to the airfoil leading edge with increasing angle of attack. The flow separated downstream of the airbrake.

The lower side was characterized by suction on its forward part, even at positive angles of attack, the stagnation point relocated from the lower side of the leading edge to its upper side. The flow on the lower side was separated even at small positive angle of attack and it did not become attached till at relatively high angle of attack of approximately +6 deg. Decreasing angle of attack at regime with the flow attached at the lower side, the separation begun at the leading edge and brusquely (during 0.1 deg decrease of the angle of attack) expanded along the whole lower side. It indicated, as pressure distribution indicated, that the stagnation point in this situation is positioned at the airfoil upper side and the flow going to the lower side is not able to overcome the leading edge without separation.

Nose-up moment was also pronounced, al-

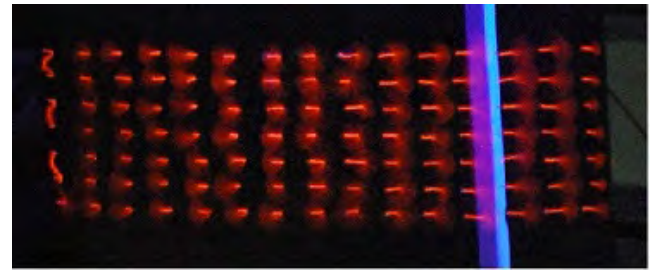


Fig. 6 Lower side, AoA 0deg

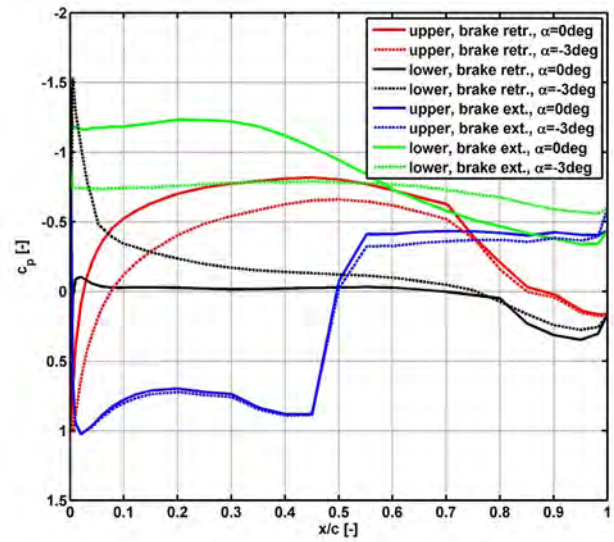


Fig. 7 Pressure distributions, zero and negative angles of attack

though the changes of pressure distribution on airfoil surfaces were in nose-down sense. It implied that the nose-up moment caused by the downstream oriented force acting on the airbrake plate prevailed over the nose-down moment caused by the changes in pressure distribution on the airfoil itself.

The lift and polar curves affirmed flow separation at angles of attack in proximity of zero or slightly negative. The negative lift did not further develop to higher absolute values with further decrease of the angle of attack, but drag increased. The pressure distributions correspondingly showed flat pressure area of negative C_p value about (-0.7), typical for flow separation, on airfoil lower side even at low positive angles of attack. It could be stated that decreasing of angle of attack with the airbrake extended caused

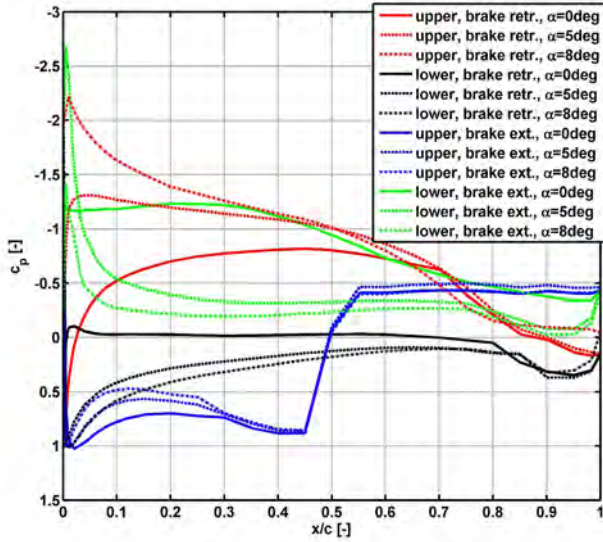


Fig. 8 Pressure distributions, zero and positive angles of attack

very early lower side separation. As this separation occurred at the positive angle of attack in proximity of zero, it could be possible to use it during flight. Airbrake performance could be increased using flight at lower angle of attack, i.e. using higher flight speed, resulting in higher descent slope of the flight path.

The moment curve of the airfoil with the deployed airbrake is of distinctly bent character indicating aerodynamic focus movement with angle of attack and lift coefficient. At typical angle of attack of 8 deg, the aerodynamic focus shifts slightly forward.

The detailed analysis of the fundamental airbrake flow physics was given in [13].

5.2 Discussion of influence of gap size

The idea arose whether the gap between the airfoil upper surface and the airbrake lower edge could increase the airbrake performance. The interest would be in simplicity of such an arrangement compared to the increasing of the height of the airbrake plate. Available airfoil height is usually limited and frequent solution with double- or triple-plate with individual plates stored one after another needs more complex mechanism and is heavier. The evident way of extension of airbrake

Table 1 Influence of gap size, airbrake plate height 93 mm (0.155 c), position 0.50 c, AoA 8deg

Gap size	0 mm	11 mm	33 mm	55 mm
Δc_L	-1.640	-1.563	-1.421	-1.346
Δc_D	0.2395	0.2661	0.3239	0.3220
$\Delta(c_L/c_D)$	≈ -70	≈ -70	≈ -70	≈ -70
Δc_m	0.0503	0.0431	0.0278	0.0328

span is not so convenient due to airfoil surface imperfections created in the area of the airbrake even by the retracted airbrake, the imperfections disturb laminar flow and thus are undesirable especially on sailplane wing.

Downstream on the airfoil upper side, a vortex developed in front of the footing of the airbrake without a gap between the airfoil and the airbrake. Strong flow separation was visible also behind the airbrake, both by PIV and the minitufts as well.

Opening of a gap resulted in appearance of stagnation point on the windward side of the airbrake plate. The flow divided and part of the air flew through the gap. The thin layer on airfoil surface remained attached even closely in front of the airbrake and behind the airbrake as well, the minitufts surface pattern was practically identical to the clean airfoil without the airbrake. The large vortex area immediately behind the airbrake was, as indicated by PIV, of the extension similar to the configuration without the gap.

Examination of the gap size between the airfoil upper surface and airbrake lower edge revealed more complex influence on global aerodynamic forces (see Tab. 1, Fig. 11, Fig. 12 and Fig. 13).

Generally, it can be stated simplified basic rule at given height of the airbrake plate. The higher the gap, the lower lift reduction but the higher drag increase. Regarding the fundamental airbrake performance expressed by the lift-to-drag ratio, increasing the gap, the drag increase equalled the higher lift in the sense that the lift-to-drag ratio remained practically identical and

very low. From this point of view, the gap did not represent any benefit. But the fact of the significantly decreased change in the moment was worth noting, as the small or none changes in aircraft trim should be desirable with the deployment of the airbrakes.

The explanation was that even small gap was hydraulically partially open to let the air flow through. It was confirmed by the visualization; the minitufts indicated attached flow on the airfoil upper side even in the close proximity of the airbrake (see Fig. 10). Consequence of open gap consisted in less abrupt changes in the airfoil pressure distributions, especially on airfoil upper side. Increasing the gap, the pressure distribution developed smoother and without abrupt sharp steps. In our testing, gap of 11 mm (0.018 of chord) has effect close to the configuration without gap, but the broader gaps really changed the pressure distribution patterns.

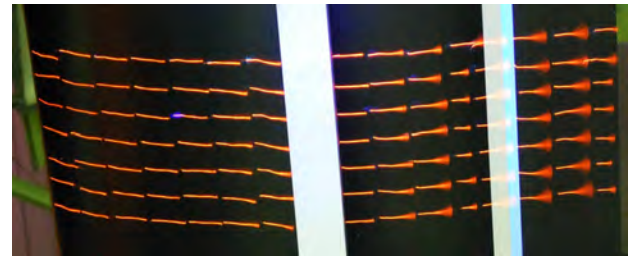


Fig. 10 Upper side, airbrake extended, gap 11 mm, AoA 0deg

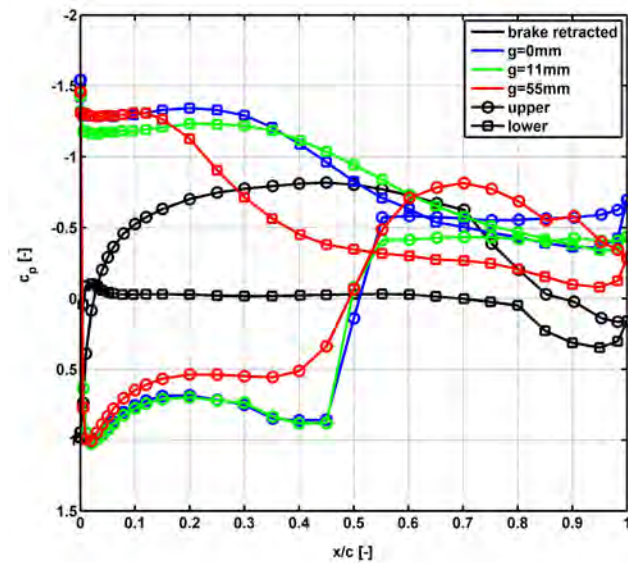


Fig. 9 Pressure distributions, AoA 8 deg

5.3 CFD Results

The configurations of the airbrake with and without the gap between airfoil and extended airbrake were calculated. The gap was 0.018 c.

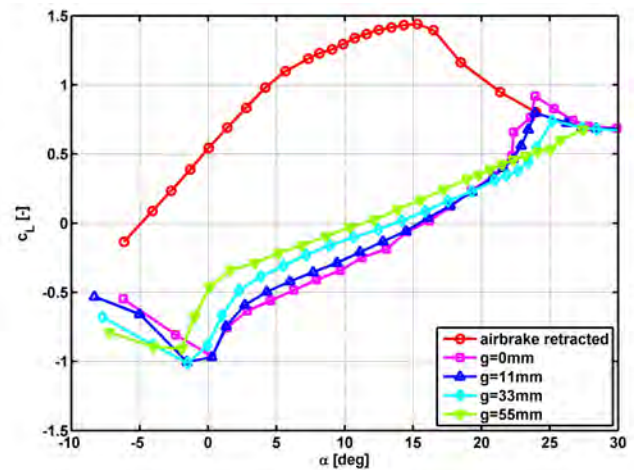


Fig. 11 Lift curves

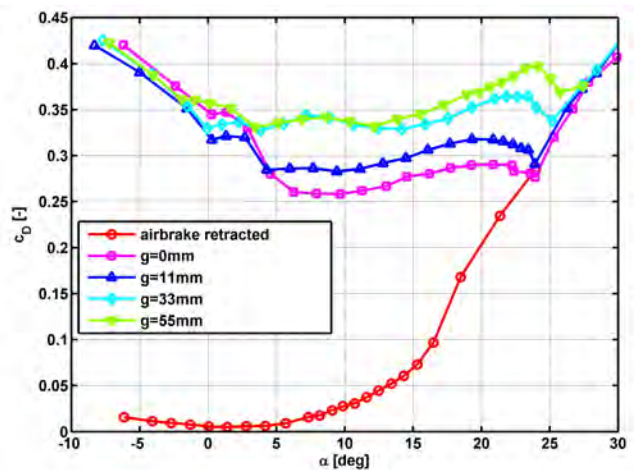


Fig. 12 Drag curves

5.3.1 Pressure distribution

The comparison of the pressure distributions around the airfoil obtained from the experiment and CFD is depicted in Fig. 14. It corresponds to the case with the gap and AoA 5deg. The

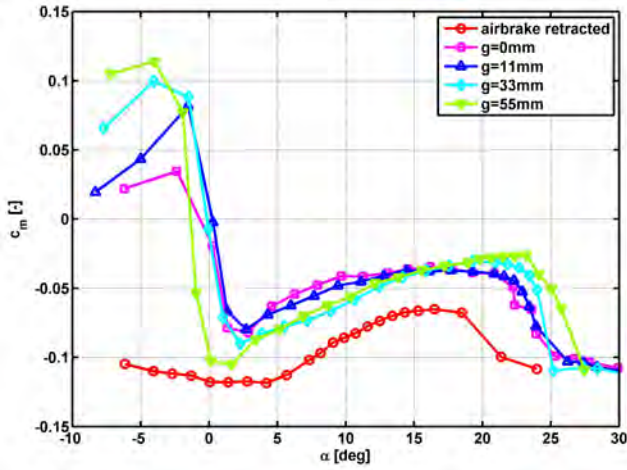


Fig. 13 Moment curves

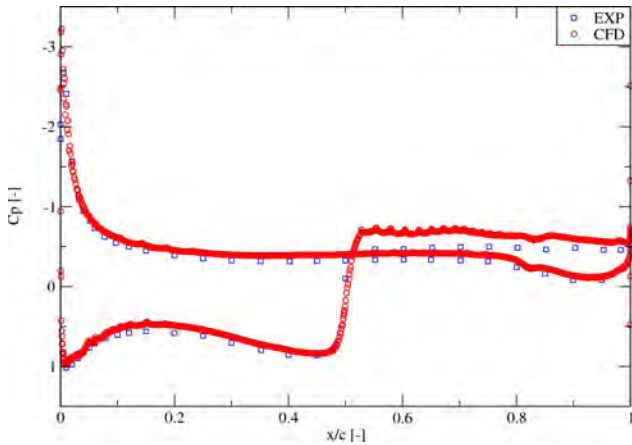


Fig. 14 Comparison of the C_p from experiment and CFD, $AoA = 5deg$

agreement between experimental and computational distribution is very encouraging. Integral force coefficients also agree quite well (C_L especially). The slightly higher suction on the lower side of the airfoil is probably caused by the rearward position of the stagnation point on the upper side of the leading edge. The higher calculated pressure downstream of the airbrake corresponds to the higher calculated drag.

5.3.2 Flowfield with and without gap

The flowfield obtained from PIV measurement during experiment is depicted in Fig. 15. It is possible to see that the calculated flowfield (see Fig. 16) is very similar with the flowfield from experiment. The measured and calculated posi-

tions of the stagnation point in the front part of the airbrake are very close to each other and the separated area of the flow above and behind the airbrake have also the same character.

The CFD confirmed that the gap was not hydraulically closed and the flow went through it (see Fig. 16). The same behaviour was observed during experiment by flow visualization by means of minitufts (see Fig. 10).

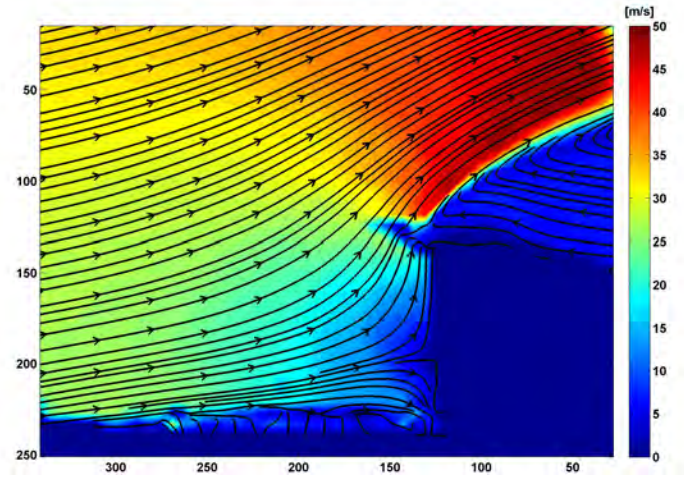


Fig. 15 Streamlines from PIV measurement upstream of extended airbrake, gap 11 mm

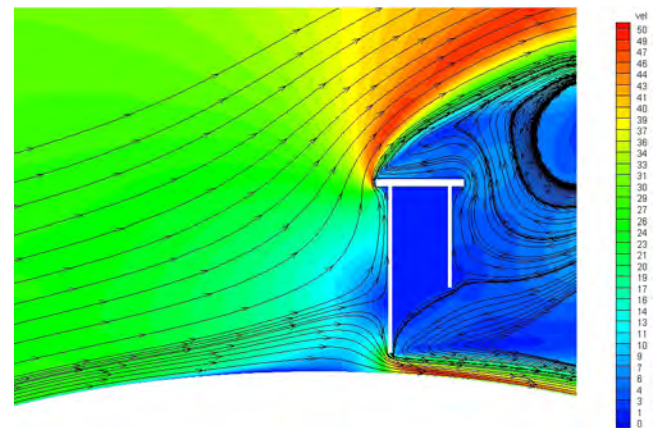


Fig. 16 Streamlines from CFD upstream of extended airbrake, gap 11 mm

The flowfields corresponding to the no gap configuration from the experiment and CFD are depicted in the Fig. 17 and Fig. 18. The flowfields have the same character from the qualitative and also quantitative point of view. The CFD slightly

overpredicted the region of the recirculating flow in front of the airbrake. The flow separation on the upper part of the gap was also captured by CFD very well.

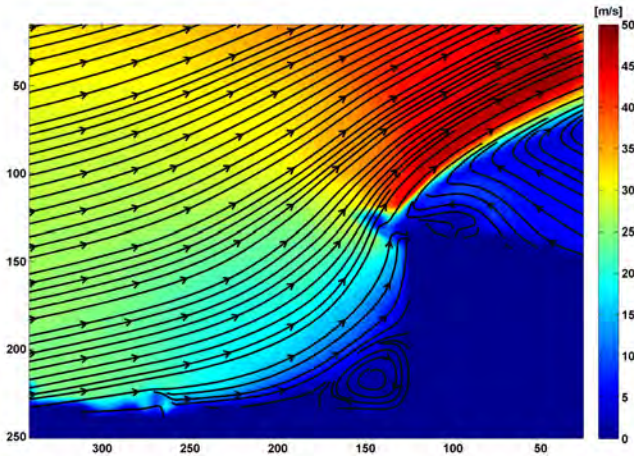


Fig. 17 PIV - upstream of airbrake, airbrake extended, gap 0

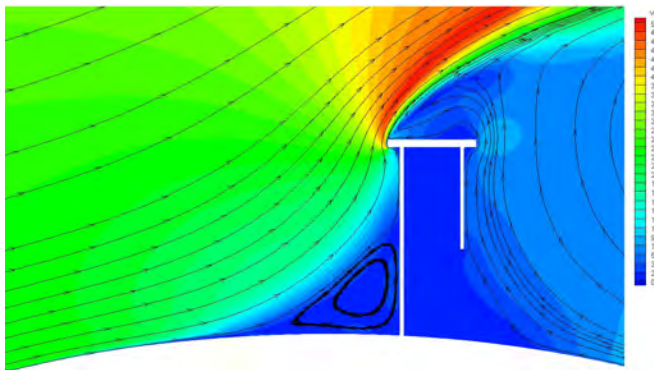


Fig. 18 CFD - upstream of airbrake, airbrake extended, gap 0

6 Conclusions

Aerodynamic performance of an airbrake and consequently airbrake capability to influence aircraft flight performance does seem to depend on geometric details of the airbrake to limited extent only. An airbrake in form of barrier on airfoil upper surface create such significant changes in airfoil flowfield that changes in height of airbrake plate, gap size between airfoil and brake and brake chordwise position in order of up 10

percents of airfoil chord are of secondary importance. So other design considerations and constraints than aerodynamic ones can be fully taken into account. If two-dimensional brake aerodynamic performance would be insufficient, the increasing of airbrake total height has been the most efficient way to increase the performance, either by increasing plate height either by increasing gap size. The evident way of extension of span is not so convenient due to airfoil surface imperfections caused by the retracted airbrake, they are disturbing laminar flow and thus undesirable mainly on sailplane wing. Similarly, shifting the brake upstream is also not convenient with similar consequence of too early laminar boundary layer transition.

Acknowledgment

The research was performed with financial institutional support from government budget through the Ministry of education, youth and sports of the Czech Republic.

References

- [1] Jacobs, H., *Luftbremsen für Segelflugzeuge, Luftwissen Band 4* . No. 7, pp. 207 - 210, 1937.
- [2] Jacobs, H., Wanner, A., *DFS Sturzflugbremsen an Segel und Motorflugzeugen*. Jahrbuch 1938 der deutschen Luftfahrtforschung, pp. I 313 – I 319.
- [3] Hoerner, S. F., *Fluid-Dynamic Drag*. Hoerner Fluid Dynamics, Bakersfield 1965
- [4] Rebuffet, P., *Aérodynamique expérimentale, Librairie polytechnique Ch. Béranger*. Hoerner Fluid Dynamics, Bakersfield 1965
- [5] Schlichting, H., Truckenbrodt, E., *Aerodynamics of the Airplane*. McGraw-Hill, New York 1979, ISBN 0-07-055341-6
- [6] Fuchs, D., *Windkanaluntersuchungen an Bremssplatten, Luftfahrtforschung Band 15* . No. 1/2, pp. 19 – 27, 1938
- [7] Davies, H., Kirk, F. N., *Résumé on Aerodynamic Data of Air Brakes* . Aeronautical Research Council R & M 2614, London 1951
- [8] Arnold, K. O., *Untersuchungen an Flügeln mit*

Bremsklappen. Zeitschrift für Flugwissenschaften, 14 (1966), No. 6, pp. 276 – 281

- [9] Pátek, Z., *Zkušební proud vzduchu v aerodynamickém tunelu Ø3 m*. VZLÚ Report R-3401/02, Praha 2002
- [10] Tyssel, L., *Hybrid Grid Generation for Complex 3D Geometries*, Proceedings of the 7th International Conference on Numeric Grid Generation in Computational Field Simulation, Whistler, British Columbia, Canada, Sept. 2000, pp. 337-346
- [11] Eliasson, P., *EDGE, a Navier-Stokes Solver for Unstructured Grids*, Proceedings to Finite Volume for Complex Applications III., ISBN 1 9039 9634 1, ISTE Ltd., London, 2002, pp 527-534
- [12] Hellsten, A., *New Advanced $k-\omega$ Turbulence Model for High Lift Aerodynamics*, AIAA Journal, Vol. 43, No. 9, Sept. 2005, pp. 1857-1869
- [13] Pátek, Z., *Wind tunnel study of an airfoil section with airbrake*. Czech Aerospace Proceedings, No.2/2012, pp. , ISSN 1211–877X

Copyright Statement

The authors confirm that they, and/or their company or organization, hold copyright on all of the original material included in this paper. The authors also confirm that they have obtained permission, from the copyright holder of any third party material included in this paper, to publish it as part of their paper. The authors confirm that they give permission, or have obtained permission from the copyright holder of this paper, for the publication and distribution of this paper as part of the ICAS2012 proceedings or as individual off-prints from the proceedings.